

1 **Performance evaluation of microbial electrochemical systems operated with**
2 **Nafion and supported ionic liquid membranes**

3
4 László Koók^{1,*}, Nándor Nemestóthy¹, Péter Bakonyi¹, Guangyin Zhen²,
5 Gopalakrishnan Kumar^{3,4}, Xueqin Lu⁵, Lianghu Su⁶, Ganesh Dattatraya Saratale⁷,
6 Sang-Hyoun Kim^{3,4}, László Gubicza¹

7
8 ¹Research Institute on Bioengineering, Membrane Technology and Energetics,
9 University of Pannonia, Egyetem ut 10, 8200 Veszprém, Hungary

10 ²School of Ecological and Environmental Sciences, East China Normal University,
11 Shanghai 200241, China

12 ³Department of Environmental Engineering, Daegu University, Gyeongsan,
13 Gyeongbuk 712-714, Republic of Korea

14 ⁴Sustainable Environmental Process Research Institute, Daegu University, Jillyang,
15 Gyeongsan, Gyeongbuk 38453, Republic of Korea

16 ⁵Department of Civil and Environmental Engineering, Graduate School of
17 Engineering, Tohoku University, Sendai, Miyagi 980-8579, Japan

18 ⁶Nanjing Institute of Environmental Sciences of the Ministry of Environmental
19 Protection, 210046, Nanjing, PR China

20 ⁷Department of Food Science & Biotechnology, Dongguk University, Ilsandong-gu,
21 Goyang-si, Gyeonggido, 410-820, Republic of Korea

22
23 *Corresponding Author: László Koók

24 Tel: +3688624385

25 Fax: +3688624292

26 E-mail: kook@almos.uni-pannon.hu

27 **Abstract**

28

29 In this work, the performance of dual-chamber microbial fuel cells (MFCs)
30 constructed either with commonly used Nafion[®] proton exchange membrane or
31 supported ionic liquid membranes (SILMs) was assessed. The behavior of MFCs was
32 followed and analyzed by taking the polarization curves and besides, their efficiency
33 was characterized by measuring the electricity generation using various substrates such
34 as acetate and glucose. By using the SILMs containing either [C₆mim][PF₆] or
35 [Bmim][NTf₂] ionic liquids, the energy production of these MFCs from glucose was
36 comparable to that obtained with the MFC employing polymeric Nafion[®] and the same
37 substrate. Furthermore, the MFC operated with [Bmim][NTf₂]-based SILM
38 demonstrated higher energy yield in case of low acetate loading ($80.1 \text{ J g}^{-1} \text{ COD}_{\text{in}} \text{ m}^{-2}$
39 h^{-1}) than the one with the polymeric Nafion[®] N115 ($59 \text{ J g}^{-1} \text{ COD}_{\text{in}} \text{ m}^{-2} \text{ h}^{-1}$). Significant
40 difference was observed between the two SILM-MFCs, however, the characteristics of
41 the system was similar based on the cell polarization measurements. The results
42 suggest that membrane-engineering applying ionic liquids can be an interesting subject
43 field for bioelectrochemical system research.

44

45 **Keywords:** bioelectrochemical system, microbial fuel cell, membrane, ionic liquid,
46 electricity generation, polarization

47

48

49 **1. Introduction**

50

51 Microbial fuel cells (MFCs) are considered as newfangled and environmental
52 friendly renewable energy-producing systems that are able to directly convert waste-
53 bound chemical energy into electricity by the assistance of electrochemically-active
54 microorganisms (Logan et al., 2006; Lovley, 2006). A classical microbial
55 electrochemical system consists of three main structural components, such as (i) an
56 anaerobic anode, (ii) an aerobic cathode chamber and (iii) a separator in-between
57 them, in most cases a membrane with ion-exchange capacity (Kumar et al., 2017). The
58 membrane, besides its role in physically separating the two half-cells, is supposed to
59 facilitate the selective transport of protons from the anode to the cathode chamber
60 (Winfield et al., 2016). So far, a significant number of studies have dealt with the
61 development of bioelectrochemical cells and it has been proven that they can be
62 operated with different type of membranes (e.g. proton exchange (PEM), anion-
63 selective, bipolar, ultra- and microfiltration or composite, etc.) (Li et al., 2011). Thus,
64 it can be concluded that their features can notably affect the performance of these
65 applications (Gildemyn et al., 2017) i.e. due to their different contribution to the
66 overall internal resistance of the system (Kumar et al., 2017). Though there is a range
67 of membranes to choose from, PEMs are the most routinely used by far (Rahimnejad
68 et al., 2014). However, their price is a factor that can limit scale-up and thus drive the
69 research to develop alternative, potential replacement materials.

70 Recently, novel membranes prepared with ionic liquids were reported as
71 promising competitors to conventional polymers such as Nafion[®] in MFCs

72 ([Hernández-Fernández et al., 2015](#)). Ionic liquids (ILs) have been recognized as novel
73 and green solvents, many of which – depending on their chemical structure – are
74 liquids even at room temperature and can be immobilized in a porous matrices to form
75 a so-called supported ionic liquid membrane (SILM) ([Bakonyi et al., 2013](#); [Bednár et](#)
76 [al., 2016](#); [Cserjési et al., 2010](#)). Moreover, there is a possibility to process the ionic
77 liquid into polymers where no porous supports are required ([Yuan et al., 2013](#)). Recent
78 findings of [Hernández-Fernández et al. \(2015\)](#) and [Hernández-Fernández et al. \(2016\)](#)
79 indicated that ionic liquids can actively participate in the proton transport taking place
80 between the anode and cathode chambers of bioelectrochemical system and
81 additionally, it was concluded that the amount of ionic liquid immobilized in the
82 membrane is able to influence the actual power output in microbial fuel cells. The
83 same research group demonstrated the role of ionic liquids in MFCs by using different
84 ionic liquid-polymer inclusion membranes (PIM) as well as ionic liquid-type
85 membrane-cathode assembly ([Salar-García et al., 2015; 2016](#)). In an interesting study,
86 [Sood and co-workers \(2015\)](#) communicated the successful combination of Nafion[®]
87 and proton conductive ionic liquids, where increasing conductivities of the doped
88 membranes along with higher ionic liquid loadings were observed. More recently, an
89 approach to prepare ionic liquid/imidazoledicarboxylic acid modified
90 poly(vinylalcohol) polyelectrolyte membranes was introduced by [Gohil and](#)
91 [Karamanev \(2016\)](#), where MFC set-ups with these blended membranes provided
92 salient current as well as power densities. Further applications of ionic liquid in MFCs
93 include (i) the functionalization of carbon nanotubes to obtain anodes with improved

94 interfacial electron transfer (Wei et al., 2016) and (ii) the modification of cathodes for
95 enhanced MFC performance (Ortiz-Martínez et al., 2016).

96 In this research work, the characteristics of SILM-based MFCs (membranes
97 prepared with [C₆mim][PF₆] and [Bmim][NTf₂] ionic liquids) were investigated in
98 terms of their main energetical traits along with behavior analysis using the
99 polarization curve technique. The results were compared to MFCs operating with
100 Nafion[®] proton exchange membrane in order to evaluate the feasibility of MFCs with
101 new generation membrane separators and attempt to deliver a better comprehension of
102 the membrane-related effects.

103

104 **2. Materials and Methods**

105

106 **2.1. Preparation of SILMs**

107

108 To prepare the SILMs, water immiscible 1-butyl-3-methylimidazolium
109 bis{(trifluoromethyl)sulfonyl}imide ([Bmim][NTf₂]) and 1-hexyl-3-
110 methylimidazolium hexafluorophosphate ([C₆mim][PF₆]) ionic liquids (IoLiTec,
111 Germany) were chosen. The main aspect was to use ionic liquids with near the same
112 hydrophobicity, thus, the effect of the hydrophobicity on the observed differences can
113 be avoided. Since the anions possess disparate hydrophobicity values, the differences
114 can be compensated through selecting the cation chain length properly. As supporting
115 layer for ionic liquid immobilization, hydrophobic porous Durapore[®] PVDF
116 membrane was used, each having a diameter of 4.5 cm, a pore size of 0.22 μm and a

117 thickness of 125 μm (Millipore Corp., USA). The SILM fabrication procedure had
118 been described in details in our previous paper (Cserjési et al., 2010). After IL
119 immobilization, the membrane surface was cleaned carefully (to remove excess ionic
120 liquid). Subsequently, the weight and thickness of the SILMs were measured and the
121 amount of IL embedded in the PVDF matrix was determined.

122

123 2.2. MFC setup

124

125 Mesophilic anaerobic sludge (with initial COD and pH of 17 g L^{-1} and 7.5,
126 respectively) collected from a local biogas plant was used for the inoculation of the
127 plexi-made MFCs which were constructed with a total working volume of 60 mL of
128 each chamber (Koók et al., 2016, Rózsenszki et al., 2015). ~~The schematic diagram~~
129 ~~of the MFC can be seen in Fig. 1.~~ The MFC chambers were separated by Nafion[®]
130 N115 (Sigma-Aldrich, USA) PEM or the different SILMs. Prior to use, the Nafion[®]
131 was pretreated by following the method described in the work of Ghasemi et al. (2013)
132 and Rahimnejad et al. (2012). Carbon cloth fixed on a titanium wire with a total
133 projected surface area of 64 cm^2 was used as electrode (both anode and cathode). The
134 cathode chamber contained 60 mL, 50 mM phosphate buffer (pH = 7), which was
135 continuously aerated. Initially, the anode chamber was filled with 45 mL of the same
136 buffer, 14 mL of the anaerobic sludge as seed source and substrates were injected in 1
137 mL volume to achieve the desired initial substrate concentration in 60 mL for the
138 experiments (see in Section 3.1.). A 100 Ω resistor was inserted in the external circuit
139 to record the potential difference between the two electrodes. More details regarding

140 the MFC set-up can be found in our earlier publications (Koók et al., 2016,
141 Rózsenszki et al., 2015, 2017). The start-up experiences with various substrate
142 (sodium acetate, glucose) feedings is discussed in Section 3.1.

143

144 **2.3. Analysis and Calculations**

145

146 The cell voltage was continuously measured and acquired by using a data
147 logger device (National Instruments). According to Ohm's law, current (I) and thus
148 other electrical data (such as current density, I or power density, P_d) could be
149 calculated based on the voltage recorded and the external resistance I . Cumulative
150 energy data I is the product of integrating the time-dependent power curve. The time-
151 specific (Y_t) and substrate-specific energy yields (Y_S) were computed according to Eqs.
152 1 and 2, respectively (specified relationships based on Koók et al., 2016;
153 Rózsenszki et al., 2015):

154

$$155 Y_t = \frac{\int_0^\tau P(t)dt}{A \tau} \quad (1)$$

156

$$157 Y_S = \frac{\int_0^\tau P(t)dt}{m_{(COD_{in})} A \tau} \quad (2)$$

158

159 where P is the power (W), A is the apparent anode surface area (m^2), τ is the operation
160 time (h) for a batch feeding cycle and $m_{(COD_{in})}$ is the amount of COD added (grams) by
161 the different substrate feedings. COD was determined in accordance with the Standard
162 Methods (APHA, 1995). The operation time was defined as the time elapsed between

163 the substrate addition and the point when the voltage peak was returned to the initial
164 value.

165 In order to measure the polarization curves (Section 3.2.), an external circuit
166 with variable resistor and a digital multimeter were applied. Based on the slope of the
167 linear region of the polarization curves, the internal cell resistance (R_i) could be
168 estimated.

169

170 **3. Results and Discussion**

171

172 **3.1. Comparing the performance of MFCs with different membrane** 173 **separators and substrates**

174

175 The SILMs were prepared successfully, having final masses of 299 mg and 296
176 mg and thicknesses of 117 μm and 115 μm in case of $[\text{C}_6\text{mim}][\text{PF}_6]$ and
177 $[\text{Bmim}][\text{NTf}_2]$ ionic liquids, respectively. The PVDF membrane pores were
178 considered saturated with the particular ionic liquid, the surface specific ionic liquid
179 contents were $11.37 \pm 0.1 \text{ mg cm}^{-2}$. This value is fairly comparable with those reported
180 by [Hernández-Fernández et al. \(2015\)](#), who manufactured SILMs with $\sim 18 \text{ mg cm}^{-2}$
181 ionic liquid content in nylon supporting layer.

182 In the first period of the MFC operation, considered as the biofilm acclimation
183 period, glucose (5 mM) as adaptation substrate was used in several consecutive cycles,
184 until stabilized current density time profiles were reached ([Carmona-Martínez et al.,](#)
185 [2015](#)). Afterwards, the main goal of the investigation was to reveal how the various

186 membrane types affect the performance of the MFC. To do so, the MFCs were
187 installed with the Nafion and SILMs and put to work with sequential feedings of 25
188 mg Na-acetate and 25 mg glucose in all cases. The main, process efficiency-related
189 parameters measured and calculated are listed in **Table 1** for comparison. From **Table**
190 **1**, it can be inferred that the MFC behavior was quite determined by the sort of
191 membrane employed, resulting in notable performance differences in case of the same
192 amount and quality of substrate. Applying acetate, the [C₆mim][PF₆]-MFC produced
193 the least attractive outputs along with the longest operation time. In summary, it can be
194 concluded that the use of [C₆mim][PF₆]-containing SILM caused 50 % lower maximal
195 voltage and current density in comparison with the Nafion[®]-MFC. In contrast, as
196 response to the same dose of acetate, the [Bmim][NTf₂]-MFC was able to exceed the
197 voltage, current and power density values of the Nafion[®]-MFC. In fact, the maximal
198 power density was 28 % higher than for Nafion[®]-MFC. Regarding glucose feeding,
199 although the [Bmim][NTf₂]-MFC was the more efficient among the two SILM-MFCs,
200 both were found to be relatively less efficient than the Nafion[®]-MFC, as both were
201 characterized with approximately 35 % lower voltage and current density outputs as
202 well as roughly 60 % less maximal power densities.

203 These achievements for the Nafion[®]-MFC coincide well with the previous
204 literature, where for instance, [Ieropoulos et al. \(2005\)](#) tested different types of MFCs
205 with pure cultures, applying Nafion[®] as separator. In case of 5 mM acetate injection
206 and absence of added mediators, the *G. sulfurreducens*-inoculated MFCs produced
207 current density values between 1.17 – 5.93 mA m⁻² and power density of 0.257 – 1.175
208 mW m⁻², meanwhile 28.5 mA m⁻² and 0.52 mW m⁻² could be achieved in our present

209 experimentation for Nafion[®] membrane. In another paper, [Chaudhuri and Lovley](#)
210 [\(2003\)](#) operated mediator-less Nafion[®]-MFCs fed with 10 mM glucose, using different
211 types of graphite anodes. They reported current densities of 28 – 74 28.5 mA m⁻²,
212 which are in the same order or magnitude with those with glucose in our present
213 Nafion[®]-MFC (36.4 mA m⁻²). In addition, [Zhang et al. \(2006\)](#) investigated MFCs with
214 perfluorinated ion membrane fed with different substrates. They reported 140 mA m⁻²
215 current density and 59 mW m⁻² power density in case of 20 mM acetate, while these
216 values were 110 mA m⁻² and 43 mW m⁻² for 10 mM glucose, respectively. Glucose
217 and acetate were also tested in our earlier work for energy generation in MFCs
218 (chambers separated by Nafion[®] membrane) inoculated with mesophilic sludge
219 ([Bélafi-Bakó et al., 2011](#)). As a response to the addition of 0.1 – 0.5 mM glucose, the
220 MFCs produced 200 – 320 mA m⁻² current and 2 – 5.1 mW m⁻² power density
221 (glucose), while after the supplementation of 0.25 – 1 mM acetate, 170 mA m⁻² and
222 1.45 mW m⁻² could be achieved ([Bélafi-Bakó et al., 2011](#)).

223 Lately, [Hernández-Fernández et al. \(2015\)](#) demonstrated that 115 mW m⁻³
224 volume specific power density could be attained by treating wastewater substrate in
225 Nafion[®]-MFC, while in contrast, the MFCs operated with [Omim][NTf₂] and
226 [Omim][PF₆]-containing nylon membranes provided 61 and 200 mW m⁻³, respectively.
227 In the light of our results with Nafion[®] (power density of 60.2 mW m⁻³ for acetate and
228 98.7 mW m⁻³ for glucose) and [Bmim][NTf₂]-based SILMs (77.2 mW m⁻³ for acetate
229 and 42.6 mW m⁻³ for glucose), it can be deduced that despite certain differences in the
230 experimental conditions (i.e. the type of cation in the ionic liquids, the support material

231 and the substrate used) the results of the current investigation agree more or less with
232 the already published literature ([Hernández-Fernández et al., 2015](#)).

233 Further description of the experiences with the various MFCs can be ensured
234 based on the energy parameters (E and Y_S). As a matter of fact, the [Bmim][NTf₂]-
235 MFC appeared to be the most reliable in the view of the obtainable (i) cumulated
236 energy and (ii) energy yield by feeding acetate. In particular, its cumulative energy
237 production was 50 % and nearly 3-fold higher than for the Nafion[®]-MFC and
238 [C₆mim][PF₆]-MFC, respectively. During the experiments, this cumulative energy
239 value was 0.41 J, while the highest energy yield of 80.1 J g⁻¹ COD_{in} m⁻² h⁻¹ could be
240 noticed. The glucose addition led to approximately the same cumulative energy values
241 for the SILM-MFCs, while the Nafion[®]-MFC produced the highest value with more
242 than 0.34 J in this part of the experiments.

243 The time course of the energy production (**Fig. 1**) suggests considerable
244 differences for the MFCs, reflecting distinguishable features between the energy
245 production kinetics of the two SILM-MFCs. The acetate-utilizing [Bmim][NTf₂]-MFC
246 was capable of reaching the peak value of the obtainable energy in 37 hours, while this
247 point could be achieved only after 100 hours of operation with the [C₆mim][PF₆]-
248 MFC. Furthermore, the [Bmim][NTf₂]-MFC significantly exceeded the performance
249 of Nafion[®]-MFC. For this latter system, the operation time was 36 hours, however, its
250 initial energy production rate gradually decreased after the 20th hour.

251 After glucose addition, the Nafion[®]-MFC was able to reach higher energy
252 values than the SILM-MFCs. Noteworthy, the [Bmim][NTf₂]-MFC showed a stable
253 energy production over 38 hours, which started to stagnate around 40 J m⁻². On the

254 other hand, stable production was followed by a slower increase after the 25th hour in
255 case of [C₆mim][PF₆]-MFC, and after 80 hours, it exceeded barely the value of
256 maximal cumulated energy produced by the [Bmim][NTf₂]-MFC at the 45th hour. It is
257 noteworthy that the MFCs were stable for more than two months (until disassembling),
258 meaning that that the membranes containing ionic liquids had no negative effect on the
259 system stability in the operational time range of this research.

260 Based on the actual efficiency obtained from g of COD fed (either in the form
261 of acetate or glucose), it can be said that the Nafion[®]-MFC produced nearly the same
262 value for the two substrates (14.3 J g⁻¹ and 13.1 J g⁻¹), while these values were 7.2 J g⁻¹
263 and 10.9 J g⁻¹ for the [C₆mim][PF₆]-MFC and 21 J g⁻¹ and 10.9 J g⁻¹ for the
264 [Bmim][NTf₂]-MFC, respectively. Accordingly, the MFC with the [Bmim][NTf₂]-
265 containing membrane possessed the highest specific energy yield for acetate (21 J g⁻¹
266 vs. 14.3 and 7.2 J g⁻¹), while nearly the same values (13.1, 10.9 and 10.9 J g⁻¹) were
267 obtained with glucose, regardless of the membrane applied.

268 Thus, it can be assumed that the [Bmim][NTf₂]-MFC had a property which
269 resulted in a more efficient acetate utilization capacity. The results cannot be explained
270 by the possible differences in the degradation capacity of the biofilms, since the same
271 cell was used in the experiments with the various membranes sequentially. Therefore,
272 the observed differences should have a relation with other intrinsic properties of the
273 biological fuel cells e.g. internal resistance, which can be influenced by the particular
274 membrane acting as an Ohmic resistance (Kumar et al., 2017). Therefore, Section 3.2.
275 presents the results of polarization curves, which were taken to see whether the change
276 of MFC internal resistances can be correlated with the membrane actually used.

3.2. Determination of the system-specific parameters: MFC internal resistance vs. membrane-type

The determination of the polarization curves (**Fig. 2**) was carried out once steady-state conditions in the MFCs (reaching the stabilized, maximum voltages) were noted with acetate substrate. Speaking generally, the Nafion[®]-MFC produced the highest current and power densities, while the results for SILM-MFCs were far below these data. The Ohmic range of the curves was twice as narrow for the SILM-operating MFCs as for Nafion[®] (up to 38 mA m⁻²), numerically up to 16 mA m⁻² for [C₆mim][PF₆]-MFC and 18 mA m⁻² for [Bmim][NTf₂]-MFC.

The maximal power density was obtained at ~ 1.5 kΩ external resistance in case of Nafion[®]-MFC, while for the SILM-MFCs, this point was reached at ~3 kΩ. The use of Nafion[®] membrane resulted in P_d value of 4.2 mW m⁻², while the [C₆mim][PF₆]-MFC produced 1.1 mW m⁻² and [Bmim][NTf₂]-MFC exceeded 1.4 mW m⁻². Based on the slope of the linear region of the polarization curves (derived from the average of at least 3 repetitions), the internal cell resistances (R_i) could be estimated (Logan et al., 2006). The R_i values for Nafion[®]-MFC, [C₆mim][PF₆]-MFC and [Bmim][NTf₂]-MFC were found as 1.3 kΩ, 2.7 kΩ and 2.5 kΩ, respectively. In case of Nafion[®], the R_i is comparable with literature data, for example, Ieropoulos et al. (2005) demonstrated acetate-utilizing (5 mM) Nafion[®]-MFC with 1.1 kΩ internal resistance. In another paper, Oh and Logan (2006) obtained R_i in the range of 89 Ω – 1.1 kΩ for acetate-utilizing Nafion[®]-MFCs, depending on the membrane size, which

299 seemed to play a defining role in the actual internal resistance of the
300 bioelectrochemical set-up.

301 Overall, it has turned out from our data that there was no significant difference
302 between the internal cell resistance of the two SILM-MFC and both of them had about
303 two times higher R_i value than the Nafion[®]-MFC. Consequently, these results imply
304 that the performance of MFCs with different membranes was not primarily associated
305 the alterations of internal resistances and it can be proposed that only a deeper study
306 on (i) properties of the individual ionic liquids as well as (ii) those of the membranes
307 prepared with them will enhance the level of understanding about the underlying
308 phenomena. This will be targeted in our next work, where parameters such as gas
309 permeability (i.e. O₂ transfer), substrate (such as acetate) transport, etc. can be useful
310 to further elaborate the MFC behaviors.

311

312 **3.3. Effect of the substrate quantity on MFC performance with supported** 313 **ionic liquid and Nafion[®] membranes**

314

315 Since the [Bmim][NTf₂]-based SILM was the most efficient with acetate,
316 further experiments were conducted using this membrane and Nafion[®] as a
317 benchmark. The effect of the amount of COD added by the substrate on the energy
318 output was studied by varying the Na-acetate loading. **Fig. 3** illustrates the tendency of
319 the cumulated energy as a function of COD added. It can be seen in the chart that E
320 values, for both membranes, were in nearly direct proportionality with the dose of
321 organic matter.

322 **Fig. 4** indicates the specific energy yields as a function of the COD input.
323 Considering the time-specific energy yield (**Fig. 4A**), it could be observed that Y_t was
324 increased by higher COD inputs using Nafion[®]-MFC. However, the [Bmim][NTf₂]-
325 MFC demonstrated a completely different tendency, as reflected by the profile
326 developed in the whole COD range studied. This stagnation may have occurred due to
327 achieving the maximal rate of the whole cell reaction, caused by possibly limited
328 (proton) transport process across the membrane and the losses related. **Fig. 4B** depicts
329 that higher energy yield could be realized at the lowest substrate loading by applying
330 the [Bmim][NTf₂]-based SILM as separator, in comparison with Nafion[®]-MFC.
331 However, this advantage rapidly disappears as the amount of substrate is increased
332 (**Fig. 4B**). Thus, it can be drawn from **Fig. 4** that in the lower substrate (acetate)
333 loading regions, SILM based on [Bmim][NTf₂] can be competitive with the widely-
334 used Nafion[®]. Nevertheless, it is an important conclusion for both the Nafion[®]-MFC
335 and the [Bmim][NTf₂]-MFC that making a trade-off between the time-specific (**Fig.**
336 **4A**) and substrate dose-specific energy yield (**Fig. 4B**) is required, since higher time-
337 specific values were manageable only at the expense of decreased substrate-specific
338 one. The observation that Y_S was in reverse relationship with substrate concentration is
339 in agreement with our previous findings on MFC operated with the liquid fraction of
340 pressed solid waste (Koók et al., 2016).

341

342

343 4. Conclusions

344

345 Supported ionic liquid membranes (SILMs) could be successfully prepared
346 using water immiscible ionic liquids and PVDF as supporting layer. Two-chamber
347 MFCs were built and operated steadily in longer-terms with Nafion[®] proton selective
348 membrane, [C₆mim][PF₆] and [Bmim][NTf₂]-based SILMs. The highest energy output
349 could be achieved with the [Bmim][NTf₂]-MFC using acetate, while the lowest one
350 was produced by the [C₆mim][PF₆]-MFC on the same substrate. In case of glucose
351 addition, the Nafion[®]-MFC was found to be the most efficient, whilst the SILM-MFCs
352 could be characterized with comparable energy generation. The assessment of
353 polarization curves led to the conclusion that the different behaviors of the two SILM-
354 MFCs (with acetate) could not be explained by the change of internal resistance (R_i)
355 values, creating a need for future study to elaborate the correlation of ionic liquid
356 properties with the actual MFC performance. The experiments on the substrate
357 loading-dependency applying acetate have shown that the [Bmim][NTf₂]-MFC could
358 be competitive with the Nafion[®]-MFC at low substrate inputs.

359 **Acknowledgement**

360

361 Péter Bakonyi acknowledges the support received from National Research,
362 Development and Innovation Office (Hungary) under grant number PD 115640. The
363 “GINOP-2.3.2-15 – Excellence of strategic R+D workshops (Development of
364 modular, mobile water treatment systems and waste water treatment technologies
365 based on University of Pannonia to enhance growing dynamic export of Hungary
366 (2016-2020))” is thanked for supporting this work. Nándor Nemestóthy was supported
367 by the ÚNKP-2016-4-04 “New National Excellence Program of the Ministry of
368 Human Capacities”.

369

370 **References**

371

372 APHA: Standard Methods for the Examination of Water and Wastewater, 19th edn.
373 American Public Health Association, New York, 1995.

374 Bakonyi, P., Nemestóthy, N., Bélafi-Bakó, K., 2013. Biohydrogen purification by
375 membranes: An overview on the operational conditions affecting the performance of
376 non-porous, polymeric and ionic liquid based gas separation membranes. *Int. J.*
377 *Hydrogen Energy* 38, 9673-9687.

378 Bednár, A., Nemestóthy, N., Bakonyi, P., Fülöp, L., Zhen, G., Lu, X., et al., 2016.
379 Enzymatically-boosted ionic liquid gas separation membranes using carbonic
380 anhydrase of biomass origin. *Chem. Eng. J.* 303, 621-626.

381 Bélafi-Bako, K., Vajda, B., Nemestothy, N., 2011. Study on operation of a microbial
382 fuel cell using mesophilic anaerobic sludge. *Desalin. Water Treat.* 35, 222-226.

383 Carmona-Martínez, A.A., Trably, E., Milferstedt, K., Lacroix, R., Etcheverry, L.,
384 Bernet, N., 2015. Long-term continuous operation of H₂ in microbial electrolysis cell
385 (MEC) treating saline wastewater. *Water Res.* 81, 149-156.

386 Chaudhuri, S.K., Lovley, D.R., 2003. Electricity generation by direct oxidation of
387 glucose in mediatorless microbial fuel cells. *Nat. Biotechnol.* 21, 1229-1232.

388 Cserjési, P., Nemestóthy, N., Bélafi-Bakó, K., 2010. Gas separation properties of
389 supported liquid membranes prepared with unconventional ionic liquids. *J. Membr.*
390 *Sci.* 349, 6-11.

391 Ghasemi, M., Daud, W.R.W., Ismail, M., Rahimnejad, M., Ismail, A.F., Leong, J.X.,
392 et al., 2013. Effect of pre-treatment and biofouling of proton exchange membrane on
393 microbial fuel cell performance. *Int. J. Hydrogen Energy* 38, 5480-5484.

394 Gildemyn, S., Verbeeck, K., Jansen, R., Rabaey, K., 2017. The type of ion selective
395 membrane determines stability and production levels of microbial electrosynthesis.
396 *Bioresour. Technol.* 224, 358-364.

397 Gohil, J.M., Karamanev, D.G., 2016. Novel approach for the preparation of ionic
398 liquid/imidazoledicarboxylic acid modified poly(vinylalcohol) polyelectrolyte
399 membranes. *J. Membr. Sci.* 513, 33-39.

400 Hernández-Fernández, F.J., de los Ríos, A.P., Mateo-Ramírez, F., Godínez, C.,
401 Lozano-Blanco, L.J., Moreno, J.I., et al., 2015. New application of supported ionic

402 liquids membranes as proton exchange membranes in microbial fuel cell for waste
403 water treatment. *Chem. Eng. J.* 279, 115-119.

404 Hernández-Fernández, F.J., de los Ríos, A.P., Mateo-Ramírez, F., Juárez, M.D.,
405 Lozano-Blanco, L.J., Godínez, C., 2016. New application of polymer inclusion
406 membrane based on ionic liquids as proton exchange membrane in microbial fuel cell.
407 *Sep. Purif. Technol.* 160, 51-58.

408 Ieropoulos, I.A., Greenman, J., Melhuish, C., Hart, J., 2005. Comparative study of
409 three types of microbial fuel cell. *Enzyme Microb. Technol* 37, 238-245.

410 Koók, L., Rózsenszki, T., Nemestóthy, N., Bélafi-Bakó, K., Bakonyi, P., 2016.
411 Bioelectrochemical treatment of municipal waste liquor in microbial fuel cells for
412 energy valorization. *J. Clean. Prod.* 112, 4406-4412.

413 Kumar, G., Bakonyi, P., Zhen, G., Sivagurunathan, P., Koók, L., Kim, S.H., et al.,
414 2016. Microbial electrochemical systems for sustainable biohydrogen production:
415 Surveying the experiences from a start-up viewpoint. *Renew. Sustain. Energy Rev.*,
416 <http://dx.doi.org/10.1016/j.rser.2016.11.107>

417 Li, W.W., Sheng, G.P., Liu, X.W., Yu, H.Q., 2011. Recent advances in the separators
418 for microbial fuel cells. *Bioresour. Technol.* 102, 244-252.

419 Logan, B.E., Hamelers, B., Rozendal, R., Schröder, U., Keller, J., Freguia, S., et al.,
420 2006. Microbial fuel cells: Methodology and technology. *Environ. Sci. Technol.* 40,
421 5181-5192.

422 Lovley, D.R., 2006. Microbial fuel cells: novel microbial physiologies and engineering
423 approaches. *Curr. Opin. Biotechnol.* 17, 327-332.

424 Oh, S.E., Logan, B.E., 2006. Proton exchange membrane and electrode surface areas
425 as factors that affect power generation in microbial fuel cells. *Appl. Microbiol.*
426 *Biotechnol.* 70, 162-169.

427 Ortiz-Martínez, V.M., Gajda, I., Salar-García, M.J., Greenman, J., Hernández-
428 Fernández, F.J., Ieropoulos, I., 2016. Study of the effects of ionic liquid-modified
429 cathodes and ceramic separators on MFC performance. *Chem. Eng. J.* 291, 317-324.

430 Rahimnejad, M, Bakeri, G., Ghasemi, M., Zirepour, A., 2014. A review on the role of
431 proton exchange membrane on the performance of microbial fuel cell. *Polym. Adv.*
432 *Technol.* 25, 1426-1432.

433 Rahimnejad, M., Ghasemi, M., Najafpour, G.D., Ismail., M., Mohammad, A.V.,
434 Ghoreyshi, A.A., et al., 2012. Synthesis, characterization and application studies of
435 self-made Fe₃O₄/PES nanocomposite membranes in microbial fuel cell. *Electrochim.*
436 *Acta* 85, 700-706.

437 Rózsenszki, T., Koók, L., Bakonyi, P., Nemestóthy, N., Logrono, W., Pérez, M., et
438 al., 2017. Municipal waste liquor treatment via bioelectrochemical and fermentation
439 (H₂ + CH₄) processes: Assessment of various technological sequences. *Chemosphere*
440 171, 692-701.

441 Rózsenszki, T., Koók, L., Hutvágner, D., Nemestóthy, N., Bélafi-Bakó, K.,
442 Bakonyi, P., et al., 2015. Comparison of anaerobic degradation processes for
443 bioenergy generation from liquid fraction of pressed solid waste. *Waste Biomass*
444 *Valor.* 6, 465-473.

445 Salar-García, M.J., Ortiz-Martínez, V.M., Baicha, Z., de los Ríos, A.P., Hernández-
446 Fernández, F.J., 2016. Scaled-up continuous up-flow microbial fuel cell based on
447 novel embedded ionic liquid-type membrane-cathode assembly. *Energy* 101, 113-120.

448 Salar-García, M.J., Ortiz-Martínez, V.M., de los Ríos, A.P., Hernández-Fernández,
449 F.J., 2015. A method based on impedance spectroscopy for predicting the behavior of
450 novel ionic liquid-polymer inclusion membranes in microbial fuel cells. *Energy* 89,
451 648-654.

452 Sood, R., Iojoiu, C., Espuche, E., Gouanvé, F., Mendil-Jakani, H., Lyonnard, S., 2015.
453 Influence of different perfluorinated anion based Ionic liquids on the intrinsic
454 properties of Nafion[®]. *J. Membr. Sci.* 495, 445-456.

455 Wei, H., Wu, X.S., Zou, L., Wen, G.Y., Liu, D.Y., Qiao, Y., 2016. Amine-terminated
456 ionic liquid functionalized carbon nanotubes for enhanced interfacial electron
457 transfer of *Shewanella putrefaciens* anode in microbial fuel cells. *J. Power Sources*
458 315, 192-198.

459 Winfield, J., Gajda, I., Greenman, J., Ieropoulos, I., 2016. A review into the use of
460 ceramics in microbial fuel cells. *Bioresour. Technol.* 215, 296-303.

461 Yuan, J., Mecerreyes, D., Antonietti, M., 2013. Poly(ionic liquid)s: An update. *Prog.*
462 *Polym. Sci.* 38, 1009-1036.

463 Zhang, E., Xu, W., Diao, G., Shuang, C., 2006. Electricity generation from acetate and
464 glucose by sedimentary bacterium attached to electrode in microbial-anode fuel
465 cells. *J. Power Sources* 161, 820-825.

466

Figure Legend

467
468
469
470
471
472
473
474
475
476
477
478
479
480

~~Fig. 1 – Schematic diagram of a dual-chamber MFC~~

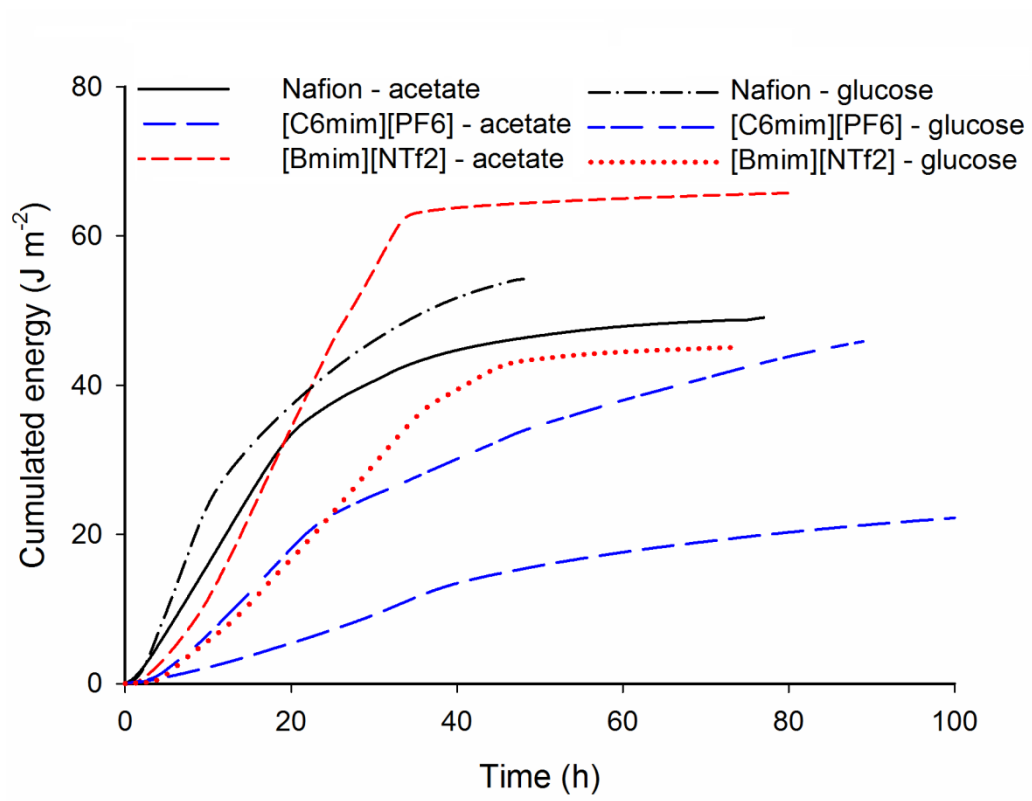
Fig. 1 – Time course of the energy production with different membranes and substrates

Fig. 2 – Results of polarization curve measurements on MFCs with various membrane separators in the presence of acetate substrate

Fig. 3 – Cumulated energy data with different acetate feedings

Fig. 4 – A: Time-specific energy yield; B: substrate-specific energy yield as a function of COD input

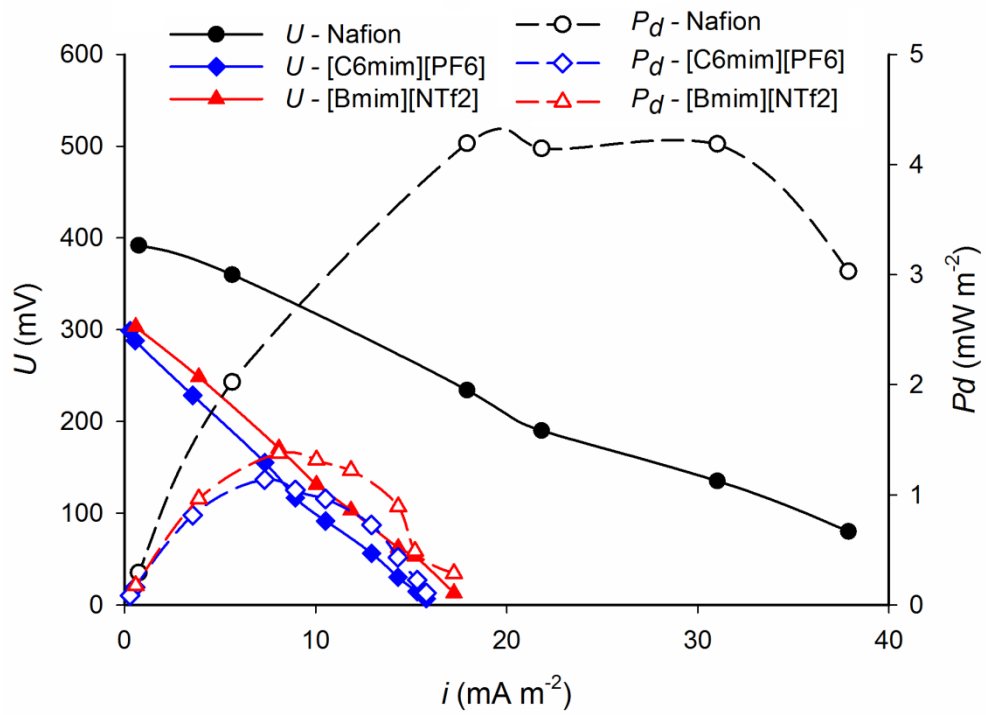
481 Fig. 1



482

483

484 Fig. 2



485

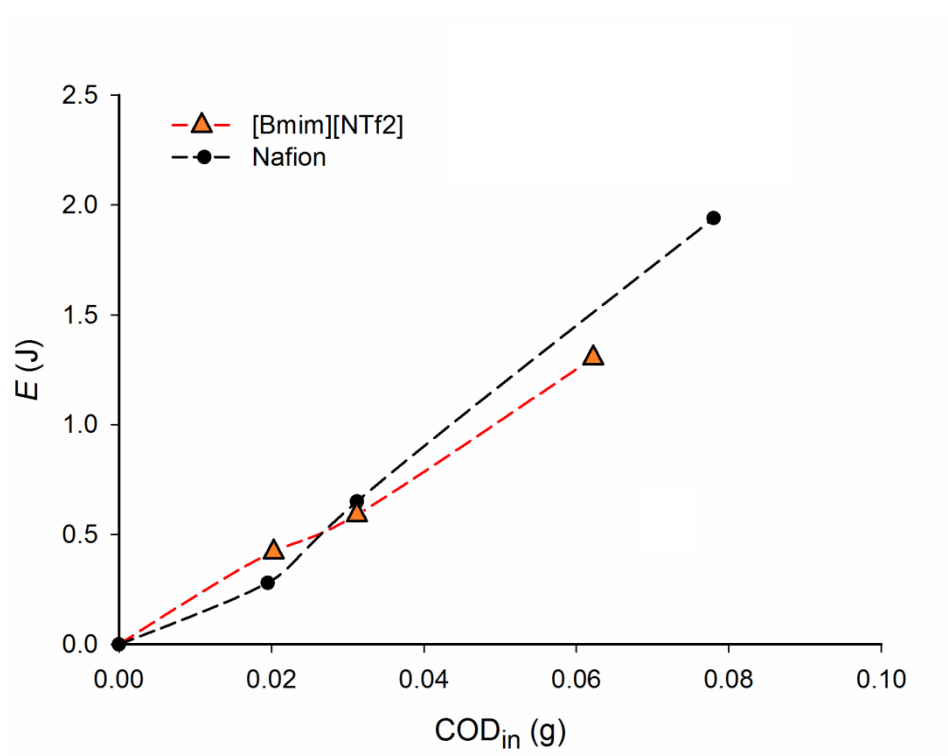
486

487

488

489

490 Fig. 3



491

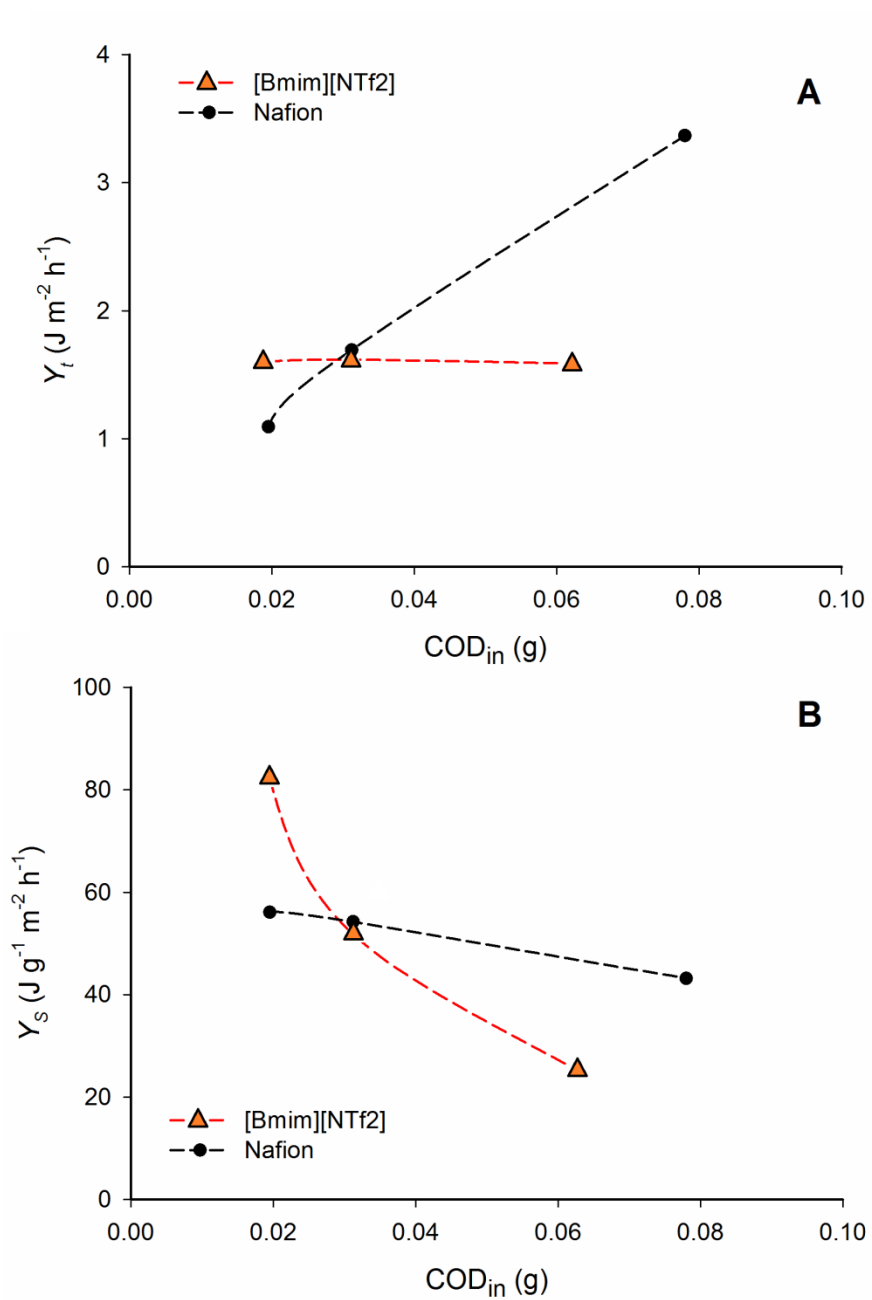
492

493

494

495

496 Fig. 4



497

498

499

500

501

502

503

504 **Table 1 – Electric outputs and operation time of substrate feedings for the**
 505 **different MFCs**

506

	Na-acetate			Glucose		
	Nafion [®]	[C ₆ mim][PF ₆]	[Bmim][NTf ₂]	Nafion [®]	[C ₆ mim][PF ₆]	[Bmim][NTf ₂]
U_{max} [mV]	18.2	9.1	20.6	23.3	14.6	15.3
i_{max} [mA m ⁻²]	28.5	14.3	32.3	36.4	22.9	23.9
$P_{d,max}$ [mW m ⁻²]	0.52	0.13	0.67	0.85	0.33	0.37
$P_{d,max}^*$ [mW m ⁻³]	60.2	15.1	77.2	98.7	38.8	42.6
τ [h]	36	97	37	42	88	41
E [J]	0.28	0.14	0.41	0.35	0.29	0.29
Y_S [J g ⁻¹ COD _{in} m ⁻² h ⁻¹]	59.0	11.4	80.1	42.2	19.2	29.5

$P_{d,max}$ and $P_{d,max}^*$ values were calculated relative to the anode surface area and the anolyte volume, respectively.

507